ARTICLES

Photodissociation of CH_2ICH_2I, CF_2ICF_2I, and CF_2BrCF_2I in Solution

Marcus Rasmusson, Alexander N. Tarnovsky, Torbjörn Pascher, Villy Sundström, and Eva Åkesson*

Department of Chemical Physics, Lund University, Box 124, 221 00 Lund, Sweden

Received: March 15, 2002; In Final Form: May 28, 2002

The photodissociation dynamics of CH_2ICH_2I, CF_2ICF_2I, and CF_2BrCF_2I have been studied in solution after excitation at 266 nm. Formation of I_2 is apparent within tens of picoseconds in solutions of CH_2ICH_2I and CF_2ICF_2I in acetonitrile, but not from CF_2BrCF_2I. More I_2 is formed from CH_2ICH_2I rather than from CF_2ICF_2I, as expected if the I_2 formation is a result of secondary dissociation of the haloethyl radicals followed by geminate combination. For CH_2ICH_2I, the I_2 formation is ultrafast (<2 ps) in several different solvents. The quantum yields of I_2 formation (after a few microseconds) were found to be 1.0 ± 0.1 for CH_2ICH_2I and 0.75−0.95 for CF_2ICF_2I in hexane, dichloromethane, and tetrachloromethane. The data on a nanosecond to microsecond time scale indicate that all haloethyl radicals decay within tens of nanoseconds. We suggest that the decay of haloethyl radicals can occur partially via abstraction.

1. Introduction

Dissociation of vicinal dihaloethanes has previously been investigated in the gas phase. Among these studies, the only time-resolved work was performed by Zewail and co-workers on CF_2ICF_2I.[1−4] Using both femtosecond and picosecond KETOF[1,2] mass spectrometry and ultrafast electron diffraction,[3,4] they discovered that upon n → σ^* excitation (promotion of the HOMO n electron of iodine to the LUMO σ^* orbital of the carbon−iodine bond), the elimination of I_2 occurs via a two-step process. An ultrafast primary (∼200 fs) C−I bond rupture is followed by a secondary carbon−iodine cleavage in the resultant $^\bullet CF_2CF_2I$ radical as a consequence of vibrational energy redistribution. This secondary dissociation occurs with an average time constant of 15−150 ps (depending on the available energy) for a fraction of the haloethyl radicals. Other important studies for understanding the dissociation of vicinal dihalides have been performed by Lee and co-workers. They used photofragment translational spectroscopy to monitor the UV photodissociation of CF_2ICF_2I,[5] CF_2BrCF_2I,[5] CH_2BrCH_2I,[5] CH_2ICH_2Cl,[6] and CF_2BrCH_2I.[7] General conclusions of their studies were that the excess energy is partitioned roughly equally between translation and internal degrees of freedom and that secondary dissociation of the haloethyl radicals often occurs due to the weakness of the β halogen−carbon bonds (with respect to the C-atom with an unpaired electron), which, however, strengthen upon fluorination.

We have chosen to study CH_2ICH_2I, CF_2ICF_2I, and CF_2BrCF_2I in solution for several reasons. First, no time-resolved measurements on the photodissociation of CH_2ICH_2I and CF_2BrCF_2I have been published previously. Second, it is of interest to examine how the vibrational energy redistribution in the $^\bullet CF_2CF_2I$ radical is affected by the presence of a solvent environment and to what extent the vibrational energy is dissipated to the solvent, because the secondary dissociation is dependent on the vibrational energy in the haloethyl radical. In principle, information on this could be obtained by comparing liquid-phase measurements with gas-phase data from the investigations of Zewail and co-workers. Third, a comparison between the systems CF_2ICF_2I and CH_2ICH_2I (and between their corresponding radicals) is motivated by the need to gain further insight into how perfluorination of haloalkanes alters their dynamical properties and stability.[8] Finally, we want to determine which processes occur after dissociation and compare this with previous studies on related systems in solution. For instance, it is of interest to examine whether an iodine−iodoethyl radical complex, $I-ICH_2CH_2$, can be formed. This complex could be regarded as an isomer analogous to H_2C-I-I (isodiiodomethane),[9,10] the formation of which we have recently observed following excitation of CH_2I_2 in solution.[11,12]

In their study of CF_2ICF_2I dissociation in the gas phase, Zewail and co-workers determined that secondary dissociation occurs for 55% of the radicals at $\lambda_{pump} = 267$ nm[4] and for only 30% at 278 nm[2] and that the process is characterized by an average time constant ∼25 ps. The dissociation of $^\bullet CH_2CH_2I$ is expected to occur faster and with a higher quantum yield, for the following reasons: (a) It is well-known that fluorination increases the branching ratio between the ground-state I($^2P_{3/2}$) and spin−orbit excited-state I*($^2P_{1/2}$) (later denoted as I/I*) by reducing the coupling between the state carrying the oscillator strength (this state correlates with I*) and other excited states[8] of iodoalkanes. Zewail and co-workers have clearly shown that haloethyl radicals created from the I* channel have less internal energy than those created from the I channel. (b) The C−I bond is weaker in $^\bullet CH_2CH_2I$ than in $^\bullet CF_2CF_2I$ due to the fact that the π bond formed concertedly upon fission of the C−I bond is stronger in the case of $^\bullet CH_2CH_2I$ (ref 5). This behavior has been attributed partially to the unusual stability of singlet CF_2 (ref 13). (c) The rate of internal vibrational energy redistribution in

* Corresponding author: Eva.Akesson@chemphys.lu.se.

10.1021/jp020720n CCC: $22.00
Published on Web 07/17/2002

$^{\bullet}CF_2CF_2I$ is probably faster than in $^{\bullet}CH_2CH_2I$ due to the higher density of states in $^{\bullet}CF_2CF_2I$.[14] The faster IVR rate would lead to a less efficient secondary dissociation if a significant part of the vibrational energy is initially deposited in the C−I bond that is not cleaved in the primary dissociation. In resonance Raman experiments on CH_2ICH_2I in cyclohexane solution with a 266 nm excitation light, a significant amount of vibrational excitation of this C−I bond stretch has indeed been observed.[15]

Other experiments also support the expectation that the lifetime of $^{\bullet}CH_2CH_2I$ is shorter than that of $^{\bullet}CF_2CF_2I$. Lee and co-workers, using photofragment translational spectroscopy to study photodissociation of CF_2BrCF_2I and CH_2BrCH_2I at 308 nm, observed stable bromoethyl radicals only from the former.[5] Wang et al., using the same technique to study photodissociation of CH_2ClCH_2Br at 266 nm, observed that a fraction of the $^{\bullet}CH_2CH_2Cl$ radicals undergoes secondary dissociation,[16] despite the fact that the C−X bond energy increases in the order I < Br < Cl.

The paper is organized as follows. Section 2 describes the experimental methods. Section 3A presents pump−probe experiments on CH_2ICH_2I, CF_2ICF_2I, and CF_2BrCF_2I in acetonitrile. A general conclusion in this section is that I_2 forms faster than 10 ps in solutions of CH_2ICH_2I and CF_2ICF_2I. We also propose a mechanism for the formation of I_2, guided by knowledge concerning the relative stability of haloethyl radicals. The formation of I_2 is further discussed in section 3B, where we present experimental results following excitation of CH_2ICH_2I in other solvents (*n*-hexane, cyclohexane, dichloromethane, and tetrachloromethane). These experiments indicate that the formation of I_2 is ultrafast (<2 ps). Other conceivable mechanisms of I_2 formation are thoroughly discussed in section 3C, where we present several arguments and experiments to distinguish between these mechanisms. In section 3D, we present and discuss the results of nanosecond experiments on CH_2ICH_2I, CF_2ICF_2I, and CF_2BrCF_2I. Femtosecond transient absorption data indicate also the formation of species other than I_2 and possible candidates are discussed in section 3E. Finally, the results and conclusions are summarized in section 3F.

2. Materials and Methods

Femtosecond pump−probe experiments were carried out using a Ti:sapphire laser/regenerative amplifier system. Pulses of 70 fs duration at 800 nm were generated by a Ti:sapphire laser operating at 82 MHz, pumped by a diode-pumped solid state laser. The pulses were amplified in a regenerative Ti:sapphire amplifier, pumped at 1 kHz by an intracavity frequeny-doubled Q-switched Nd:YLF laser. The amplified pulses typically had an energy of ∼0.9 mJ and a duration ∼100 fs. About 35% of the amplifier output was used to generate the 266 nm excitation light in a frequency tripler. The remaining 65% of the amplifier output was used directly or after attenuation to generate probe light, either as quasi-monochromatic light or as a white-light continuum. In the first case, an OPA was employed. In the latter case, light at 800 nm was first frequency-doubled to 400 nm using a 1.5 mm thick KDP crystal and then used for generation of continuum probe light pulses by focusing into a 5 mm sapphire plate. The plane of polarization of the pump beam could be varied with a Berek polarization compensator and that of the probe beam was purified using a Glan-Thomson polarizer. Unless stated otherwise, the relative polarization of the beams was set to the magic angle. Before interaction with the sample, the analyzing light was split into reference and probe beams. After passing the sample and a monochromator, these beams were registered separately by the probe and reference photodiodes. In the sample position, the excitation beam was focused using a $f = 150$ mm lens and overlapped with the probe beam focused using a $f = 75$ mm lens. The angle between the beams was ∼10° to reduce the contribution to the transient absorption signal from the front window of the sample cuvette. The excitation pulse had ∼140 fs temporal width (fwhm) and delivered typically 5 μJ in energy to a spot of variable diameter in the range 170−250 μm at the sample position. The changes in optical density of the sample (ΔA) were detected using a scheme described previously in ref 17, and some recent refinements of the detection system are discussed in refs 18 and 19. The sample was pumped through a 1 mm (unless stated otherwise) Spectrosil quartz flow cell with 1.25 mm thick walls. In all kinetic traces, a sharp feature was observed at $t = 0$. This feature was also observed in neat acetonitrile (and in the other neat solvents such as tetrachloromethane, dichloromethane, cyclohexane, and *n*-hexane, used in section 3B). We assign this solvent signal to induced phase modulation,[20,21] although excited-state absorption and two-photon absorption[19] may also contribute (front window contribution to the overall signal was negligibly small, even at $t = 0$). This sharp feature was used to determine zero time delays between pump and white light probe pulses at different wavelengths (the dispersion curve). For measurements of transient spectra, the delay line was moved automatically in accordance with the predetermined dispersion curve in order to account for the difference in arrival times of different spectral components of the continuum.

In section 3E, we present measurements obtained with a nanosecond laser flash photolysis setup. Briefly, the pump beam at 266 nm was obtained by quadrupling the output from a Nd:YAG laser. The probe light from a Xenon arc lamp was focused to a 1 mm diameter spot overlapping the unfocused pump beam with a diameter of 2.5 mm. The peak intensity of the pump pulse was estimated to be $\sim 2.5 \times 10^{10}$ W/m^2. After the 1 mm path length Spectrosil quartz flow cell containing the sample, the probe light was passed through two single monochromators and detected by a photomultiplier tube (PMT). The signal from the PMT was amplified by a 400 MHz amplifier and digitized with 500 ps/data point. The time resolution is not only determined by the pulse length (fwhm 10 ns) but also by the digitizing and the signal-to-noise ratio; we estimate it to be ∼20 ns.

All solvents used were received from Merck and were of p.a. quality. The solutions were bubbled with argon prior to the experiments. CH_2ICH_2I (>97%) was purchased from Fluka and CF_2ICF_2I (97%) and CF_2BrCF_2I (97%) were purchased from Larodan Fine Chemicals. I_2, the major contamination in CH_2ICH_2I, was due to thermal degradation of CH_2ICH_2I and probably present in a higher amount than specified, as seen by the strong coloring of the sample. It should be mentioned that the study of molecules that form iodine upon dissociation involves some complications in acetonitrile due to the fact that I_2 undergoes photoaccelerated reactions with this solvent[22] on longer time scales. The result of the reactions is formation of I_3^-, which has an absorption maximum at 362 nm[23] with $\epsilon = 27\,300$ M^{-1} cm^{-1}. $[CH_3CN{\cdot}I]^+$ has been proposed as the counterion.[22] Transient absorption kinetics recorded on old solutions of CH_2ICH_2I had a bleach contribution at 360 nm, which was not observed in fresh samples. To minimize this problem, we purified the CH_2ICH_2I from I_2 prior to use by washing with 2-propanol followed by drying in an argon flow. The measurements presented in the section 3B using solvents other than acetonitrile were performed on solutions of non-

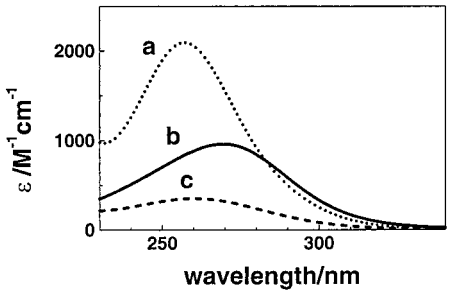

Figure 1. Absorption spectra of (a) CH_2ICH_2I, (b) CF_2ICF_2I, and (c) CF_2BrCF_2I in acetonitrile.

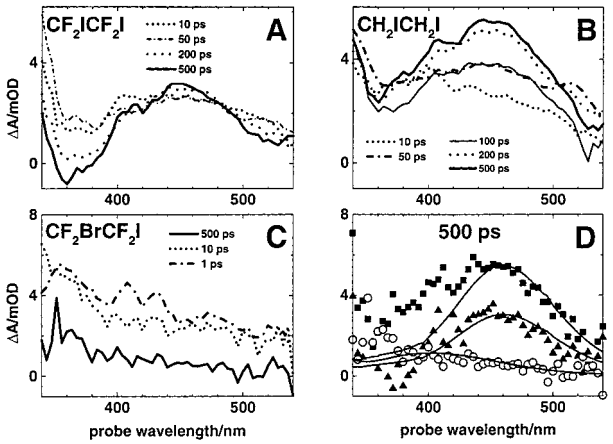

Figure 2. Transient spectra in acetonitrile. The samples were circulated through the flow cell of path length 0.5 mm with unity absorbance at 266 nm for all three compounds. Accordingly, the used concentrations were 12 mM CH_2ICH_2I, 28 mM CF_2ICF_2I, and 57 mM CF_2BrCF_2I. The used excitation intensity was 6.3×10^{14} W/m^2. For comparison with time-resolved data, steady-state spectra of I_2 (maximum at 455 nm) and IBr (maximum at 400 nm) are shown in panel D, where the spectra of I_2 are scaled to coincide with the low-energy parts of the transient spectra of CH_2ICH_2I (solid squares) and CF_2ICF_2I (solid trangles). The IBr spectrum is scaled to coincide with the low-energy part of the transient spectrum of CF_2BrCF_2I (open circles).

purified CH_2ICH_2I. Control experiments performed on an *n*-hexane solution of I_2 (0.25 g/L) proved that the signals observed in the CH_2ICH_2I solutions were not due to direct excitation of the 3% (0.09 g/L) I_2 present as impurity. CF_2ICF_2I and CF_2BrCF_2I were used without further purification because of the lower level of contamination. Steady-state spectra were measured using a JASCO V/530 UV/vis spectrophotometer.

3. Results and Discussion

A. CH_2ICH_2I, CF_2ICF_2I, and CF_2BrCF_2I in Acetonitrile. Steady-state absorption spectra of CH_2ICH_2I, CF_2ICF_2I, and CF_2BrCF_2I in acetonitrile are shown in Figure 1, and transient absorption spectra of these molecules in acetonitrile after excitation at 266 nm are shown in Figure 2.[24] The excitation energy and the optical density at the excitation wavelength were identical for the three compounds in order to ensure the same concentration of excited species. With increasing time delay, an increase of the transient absorption is observed in the spectral region 440−800 nm in the solutions of CH_2ICH_2I and CF_2ICF_2I. We assign this to formation of I_2, which in acetonitrile has an absorption maximum at 455 nm, as also shown in Figure 2 panel D. The I_2 formation occurs much faster than 10 ps. The ensuing spectral evolution observed at time delays below 200 ps can then be partly attributed to vibrational relaxation (and/or excited-state dynamics) of molecular iodine. However, because no previous studies of these issues for I_2 in acetonitrile are available, the complete assignment of the signal at earlier times remains at present uncertain and will be discussed in later sections. Figure 2 also demonstrates that in the blue part of the time-resolved spectra, I_2 is not the only species contributing to the transient absorption for CF_2ICF_2I at short delay (panels A and D) and for CH_2ICH_2I at both short and long delays (panels B and D). The possible assignments will be discussed in section 3E.

As evident from the transient spectra, the yield of I_2 is highest in the case of CH_2ICH_2I, whereas the I_2 formation is less efficient for CF_2ICF_2I and seemingly absent for CF_2BrCF_2I. We suggest the following explanation to this trend. It is well-known from gas phase studies that excitation of all three compounds at 266 nm leads to their dissociation into haloethyl radicals and atomic iodine. Because no major differences between the absorption spectra in the gas phase and solution exist, the same dissociation process most likely occurs also in solution. The haloethyl radicals are initially internally excited and could therefore undergo secondary dissociation of the remaining β carbon−halogen bond. For reasons explained above, $^{\bullet}CH_2CH_2I$ is expected to have a shorter lifetime than $^{\bullet}CF_2CF_2I$. Because carbon−iodine bonds are generally weaker than carbon−bromine bonds, we expect the lifetimes of both $^{\bullet}CH_2CH_2I$ and $^{\bullet}CF_2CF_2I$ to be shorter than that of $^{\bullet}CF_2CF_2Br$. In solution, the yield of secondary dissociation might be lower than in the gas phase due to vibrational cooling, which for neutral polyatomic molecules in solution typically occurs on time scales from a few picoseconds to hundreds of picoseconds,[14,25,26] i.e., on a time scale similar to that of secondary dissociation of CF_2ICF_2I in the gas phase. However, it is unlikely that vibrational energy transfer to the solvent will completely suppress secondary dissociation, because the distribution of internal vibrational energy in the haloethyl radicals is fairly broad.[1,2] Atoms that have been formed from the same parent molecule may combine geminately to I_2 (in solutions of CH_2ICH_2I and CF_2ICF_2I) or IBr (in solutions of CF_2BrCF_2I). In the same solvent, we would expect the yield of I_2 to be highest for CH_2ICH_2I, smaller for CF_2ICF_2I (due to its more persistent haloethyl radical), and smallest for CF_2BrCF_2I (for which only nongeminate combination of cage escaped iodine atoms can occur). If secondary dissociation occurs for CF_2BrCF_2I, IBr formation might follow. Even if the amount of IBr formed upon photolysis of CF_2BrCF_2I would be as high as the amount of I_2 formed from CF_2ICF_2I, a contribution of IBr to the transient absorption should be less significant due to its relatively small extinction coefficient. In acetonitrile, IBr was measured to have an absorption maximum at 401 nm with $\epsilon = 370$ M^{-1} cm^{-1} whereas I_2 has $\epsilon = 860$ M^{-1} cm^{-1} at 455 nm. Both transitions are due to the molecular halogen:CH_3CN charge-transfer complexes.[22] A comparison between the transient absorption in the CF_2BrCF_2I solution and the steady-state spectra of IBr and I_2 (Figure 2) shows that the main contribution to the transient absorption could be due to IBr whereas any contribution from I_2 is negligible. In principle, other mechanisms for I_2 formation than the one proposed above could be possible. This issue is discussed further in section 3C.

Kinetic traces of CH_2ICH_2I, CF_2ICF_2I, and CF_2BrCF_2I in acetonitrile at 440 nm are shown in Figure 3. The measurements were performed with the relative pump−probe polarizations at the magic angle, and with the optical density at the excitation wavelength identical for the three compounds in order to ensure the same concentration of excited species. The traces exhibit a sharp solvent spike at $t = 0$ followed by absorption changes

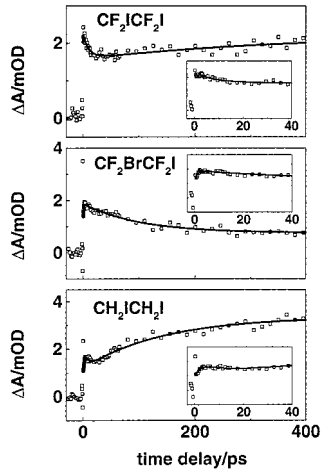

Figure 3. Kinetic traces (symbols) in acetonitrile measured at 440 nm. The intensity was 6×10^{14} W/m^2 and the concentrations were 21 mM (CF_2ICF_2I), 57 mM (CF_2BrCF_2I), and 11 mM (CH_2ICH_2I). Due to a strong solvent contribution to the measured transient absorption signal at zero delay time, kinetic analysis of the data was performed for time delay >0.5 ps and the best fits are shown by thick lines.

TABLE 1: Kinetic Parameters Determined from the Analysis of Transient Absorption Data of CH_2ICH_2I, CF_2ICF_2I, and CF_2BrCF_2I at 440 nm in Acetonitrile Using the Function $F(t) = \sum_{i=1}^{3}[A_i \exp(-t/\tau_i)] + A_4$

compound	A_1[a]	τ_1 (ps)	A_2	τ_2 (ps)	A_3	τ_3 (ps)	A_4
CH_2ICH_2I	−0.23	2.5	0.19	5.5	−0.23	150	0.35
CF_2ICF_2I	−0.18	2.9	0.26	6.0	−0.14	400	0.42
CF_2BrCF_2I	−0.46	0.9	0.05	4.0	0.29	110	0.2

[a] Amplitudes were normalized such that $\sum|A_i| = 1$. Negative and positive amplitudes represent rising and decaying components, respectively. A time constant of 10 000 ps was included to represent a persistent offset on the transient absorption signal at long delays. Error bars correspond to 15% of the parameter value.

similar to those seen in the time-resolved spectra (Figure 2) for delays longer than 10 ps. The kinetics could be fitted using three exponential functions, namely a few picosecond rise and decay followed by a much slower picosecond process, and a persistent offset at long delays. The kinetic parameters of the best fits (as judged by the χ^2 value) are given in Table 1. The transient absorption signal at this probe wavelength is mainly due to I_2 and other species, whose spectral assignments will be further discussed in section E.

The quantum yield of formation of molecular iodine could be estimated using the ΔA signal at the delay 200 ps as a measure of the I_2 concentration and the isomer of CH_2I_2 (H_2C-I-I) as a transient actinometer ($\Phi_{iso} = 0.7$;[12] Standard deviation of the mean is ±0.15). Samples of CH_2I_2 and CH_2ICH_2I, CF_2ICF_2I, and CF_2BrCF_2I in acetonitrile were prepared with the same absorbance at 266 nm and transient absorption spectra were measured in identical conditions. The maximum transient signal of H_2C-I-I at 390 nm ($\Delta A_{H_2C-I-I} = 0.065$), and the transient signals of CH_2ICH_2I and CF_2ICF_2I at 455 nm were substituted into eq 1 for the determination of Φ_{I2}. The extinction

$$\frac{\Delta A_{I_2}(\lambda)}{\Delta A_{H_2C-I-I}(\lambda)} \frac{\epsilon_{H_2C-I-I}(\lambda)}{\epsilon_{I_2}(\lambda)} \Phi_{iso} = \Phi_{I_2} \qquad (1)$$

value of 5600 M^{-1} cm^{-1} was used for H_2C-I-I (ϵ_{H_2C-I-I}) at 390 nm.[12] The quantum yields Φ_{I_2} thus obtained were 0.40 and 0.25 for CH_2ICH_2I and CF_2ICF_2I, respectively. In a similar manner, a yield of 0.17 was obtained for the formation of IBr from CF_2BrCF_2I at 500 ps.

The unity or very close to unity quantum yield for the primary C−I bond breaking is suggested for the parent compounds.[1,5,8,27,28] The calculated rate of diffusion-controlled combination of cage escaped iodine atoms is approximately 20 ns at our concentrations and excitation energy and thus not responsible for the observed formation of I_2 on the femtosecond to picosecond time scale of this experiment.[29] The obtained Φ_{I2} values of 0.25 and 0.40 for CH_2ICH_2I and CF_2ICF_2I show that at least this fraction of the haloethyl radicals rapidly loses a second I atom. For $^{\bullet}CF_2BrCF_2$, the secondary dissociation is the least pronounced among the studied compounds. The rate of appearance of I_2 absorption depends on both the rate of I_2 formation (combination of iodine atoms) and the rate of the subsequent vibrational relaxation. The latter process has not been studied separately in acetonitrile. Some increase of the I_2 absorption from 200 to 500 ps in CH_2ICH_2I and CF_2ICF_2I sample (see Figure 2) suggests that the vibrational relaxation indeed may be slow and, therefore, the obtained Φ_{I2} values are low limits. To determine the mechanisms leading to ultrafast I_2 formation (as discussed above), we have studied the dissociation dynamics of CH_2ICH_2I in other solvents where a comparison with previous studies of vibrational relaxation of I_2 is possible (see section 3B).

B. Iodine Formation from CH_2ICH_2I in Other Solvents. Pump−probe experiments on CH_2ICH_2I in solvents other than acetonitrile were performed in order to investigate whether evidence for fast I_2 formation could be obtained. Photodissociation of I_2 in the condensed phase has been studied by many authors (we refer to recent work[30] for references). Particularly relevant to us are the pump−probe studies of the photodissociation of I_2 ($\lambda_{exc} = 590$ nm) and its geminate recombination in several commonly used solvents (but not acetonitrile) performed by Harris and co-workers.[31−34] Their work[31,32] contains kinetic traces (at 635 and 710 nm) that reveal the dynamics of predissociation from the *B* state to repulsive states, subsequent trapping/detrapping in the excited *A*/*A*′ states and vibrational relaxation in the ground state.[34] Because the *A*/*A*′ states and the ground state are degenerate in the asymptotic limit, the two latter processes will occur also when I_2 is formed following excitation of CH_2ICH_2I. Therefore, a comparison between the kinetic traces in the work of Harris and co-workers and kinetic traces of CH_2ICH_2I in the same solvents could provide information on the rate and dynamics of I_2 formation following 266 nm excitation of CH_2ICH_2I.

We examined the dynamics of I_2 formation following excitation of CH_2ICH_2I in *n*-hexane, cyclohexane, tetrachloromethane, and dichloromethane. The steady-state absorption maximum of I_2 in these solvents is positioned at 520, 515, 513, and 505 nm, respectively.[35] Kinetic traces at 520, 635, and 710 nm are shown in Figure 4, both for the neat solvents and for the CH_2ICH_2I solutions. Due to two-photon absorption, the excitation light at 266 nm gives rise to a relatively strong transient absorption in the neat solvents. To a large extent, this is suppressed in the CH_2ICH_2I solutions by solute absorption. To estimate the contributions due to excitation of ICH_2CH_2I only, we first assumed that the transient absorption at ~1 ps was entirely due to the solvent. Then, the accordingly scaled traces of the neat solvents[36] were subtracted from the traces measured in the CH_2ICH_2I solutions. The assumption is justified by the slow rates of appearance of I_2 in the *A*/*A*′ states or in the ground state (most likely the only other contribution at these wavelengths) observed by Harris and co-workers.

The positive rise observed in *n*-hexane at 520 nm (where I_2 has an absorption maximum), shown in Figure 4A, is due to

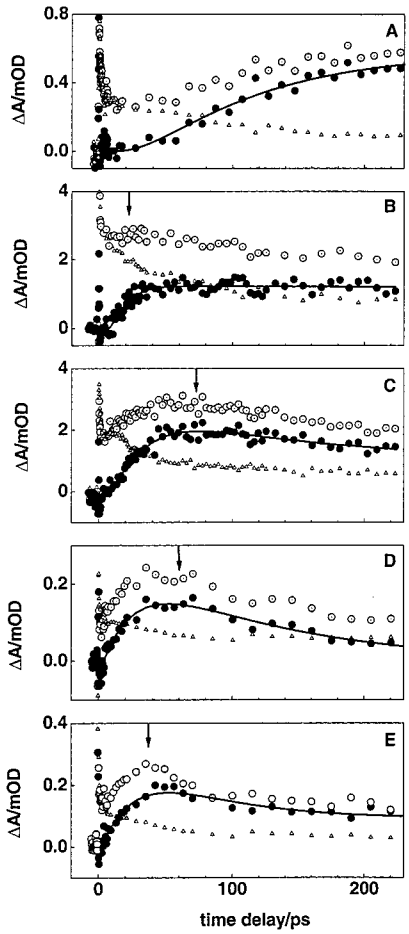

Figure 4. Transient absorption of 1,2-diiodoethane (filled circles) obtained by subtracting the transient absorption of neat solvents (open triangles), scaled as described in the text, from the transient absorption of solutions of 1,2-diiodoethane (dotted circles): (A) *n*-hexane 520 nm; (B) dichloromethane 710 nm; (C) tetrachloromethane 710 nm; (D) cyclohexane 635 nm; (E) *n*-hexane 635 nm. The amplitudes should not be directly compared due to the use of different excitation intensities and concentrations (10−29 mM). The excitation wavelength was 266 nm. The scaling factors for the solvents were 0.29 (A), 0.46 (B), 0.35 (C), 0.20 (D), and 0.04 (E); see ref 36 for details. Thick lines represent fits to the data for time delay longer than 1 ps. Arrows indicate the delay times, at which the transient absorption maxima were observed in refs 31 and 32.

formation of I_2 after photolysis of CH_2ICH_2I.[37] We also performed measurements on CH_2ICH_2I in dichloromethane and tetrachloromethane at 710 nm (Figure 4B,C) and in cyclohexane and *n*-hexane at 635 nm (Figure 4D,E). These kinetic traces exhibit rises on the picosecond time scale, followed by slower decays (tens of picoseconds). A similar behavior was observed in the study of I_2 photodissociation by Harris and co-workers, who assigned the induced absorption at these wavelengths to I_2 trapped transiently in the A/A' state (main contribution) and vibrationally hot I_2 in the ground state (minor contribution). For comparison, we indicate by arrows in Figure 4 the times at which maxima were observed in the work of Harris and co-workers. The fact that maxima are observed at these wavelengths also in solutions of CH_2ICH_2I, and even at very similar time delays, suggests that the dominating mechanism for I_2 formation in these solvents is an ultrafast process. More precisely, the formation occurs largely within a time delay comparable to the time required for the B state predissociation and geminate recombination. These processes are essentially completed within 2 ps.[33,34] We conclude that I_2 formation following excitation of CH_2ICH_2I largely occurs within a few picoseconds, most likely by the geminate mechanism proposed in section 3A.

The decays in Figure 4 are less pronounced than the corresponding decays in the study of Harris and co-workers. We attribute this to two causes. First, there is most likely a relatively broad range of formation times of I_2 after excitation of CH_2ICH_2I. Second, because I_2 is generated via excitation of CH_2ICH_2I in our experiments, a residual positive signal will persist for as long as a population of I_2 exists at wavelengths of I_2 absorption. In contrast, in the experiments of Harris and co-workers, the complete recovery of I_2 in its ground state will bring the transient absorption to zero.

C. Discussion of the Mechanism Leading to Fast I_2 Formation. As shown in section 3A, the amount of I_2 formed within 500 ps upon photolysis of vicinal dihaloethanes in acetonitrile is largest for CH_2ICH_2I, smaller for CF_2ICF_2I, and negligible for CF_2BrCF_2I. For the latter compound, the transient spectrum indicates formation of IBr. This trend in the behavior of the vicinal dihaloethanes is what would be expected if secondary dissociation followed by combination of iodine atoms were the mechanism producing I_2, because the stability of the haloethyl radicals is thought to decrease in the order $^{\bullet}CF_2CF_2$-Br > $^{\bullet}CF_2CF_2I$ > $^{\bullet}CH_2CH_2I$. The observation of fast I_2 formation from CH_2ICH_2I in different solvents, as concluded from the measurements presented in section 3B, is also in accordance with such a mechanism. However, the experimental evidence presented in sections 3A and 3B alone does not exclude the parallel occurrence of other mechanisms that could lead to fast production of I_2, e.g., cluster-dependent mechanisms and photodissociation of the haloethyl radicals. In this section, we will therefore take these possibilities into account.

Considering the relatively high concentrations used in the experiments (e.g., in the measurements presented in Figure 2 we used concentrations of a few tens of millimolar) one could suspect that there might be a tendency for the molecules to form clusters. The dimerization of a simple haloalkane, CH_3I, in the gas phase within a broad range of pressure and temperature was proposed in ref 38 but questioned in ref 39. Dimer structures have been proposed for CH_3I clusters in the molecular beam/supersonic jet and it has been shown that photodissociation of the CH_3I clusters in the A-continuum leads to formation of molecular iodine.[40−43]

Observation of I_2 formation after excitation of neat CH_3I solutions has been interpreted as resulting from excitation of CH_3I molecules in clusters.[44] The mechanisms that have been considered for I_2 formation in CH_3I clusters in the gas-phase are either sequential or concerted.[42]

$$\text{sequential: } CH_3I + h\nu \rightarrow {}^{\bullet}CH_3 + I^{\bullet}$$

$$[CH_3^{\bullet} + I^{\bullet}\cdots ICH_3] \rightarrow I_2 + 2CH_3^{\bullet}$$

$$\Delta H = -0.23 \text{ eV for I*}$$

$$\text{concerted: } [CH_3I\cdots ICH_3] + h\nu \rightarrow I_2 + 2CH_3^{\bullet}$$

$$\Delta H = -1.62 \text{ eV for } \lambda_{exc} = 266 \text{ nm}$$

The following observations indicate that clustering of the vicinal dihaloethanes do not play any major role for the formation of I_2 in the present study. First, I_2 formation via the concerted mechanism is known to result in ground-state I_2 with very little excess vibrational energy.[40] In contrast, our results in section 3B suggest that I_2 is initially formed vibrationally hot and not only in the ground state, similar to the case when it is formed as a result of recombination following photodissociation of I_2.

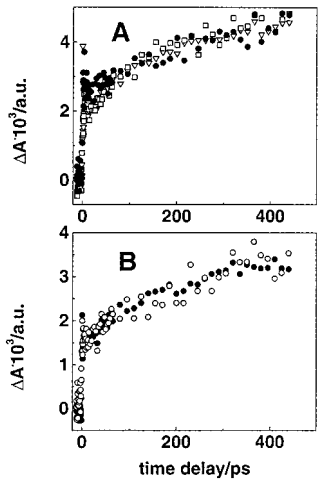

Figure 5. Concentration dependence at constant excitation intensity (A) and excitation intensity dependence at fixed concentration (B) of 1,2-diiodoethane kinetics in acetonitrile at $\lambda_{pump} = 266$ nm and $\lambda_{probe} = 440$ nm. In (A), the concentrations were 3.5 mM (filled circles), 12 mM (open squares), and 26 mM (open triangles). The intensity was 1.7×10^{15} W/m^2. In (B), the intensities were 1.8×10^{14} W/m^2 (open circles) and 1.1×10^{15} W/m^2 (filled circles). The concentration was 12 mM. The kinetic traces were scaled to coincide for longer time delays.

Second, I_2 formation via a sequential mechanism is exothermic only for iodine atoms in the excited spin−orbit state, I*. Because I* formation is dominant only for the primary dissociation of perfluorinated CF_2ICF_2I,[1,8,27] the yield of I_2 would be highest for this compound if the sequential mechanism were dominating. Third, a tendency of the molecules to form clusters should be detectable as perturbations of the UV−vis steady-state spectrum as the concentration is altered. Dimerization of CH_3I in the gas phase was concluded on the basis of a gradual blue shift and increasing asymmetry of the A-band absorption when CH_3I concentration increased.[38,45] We have measured spectra of CH_2ICH_2I in 2-propanol in the concentration range 0.6−9 mM. No alteration of the spectrum was observed, suggesting that the propensity for clustering of vicinal dihaloethanes in solution is too weak to be of importance in our pump−probe experiments. The choice of 2-propanol was motivated by the poor solubility of CH_2ICH_2I in this solvent. The solubility of CH_2ICH_2I in the solvents used in the pump−probe experiments was higher than in 2-propanol by the following factors: acetonitrile, 3.7; tetrachloromethane, 8.2; dichloromethane, 11.7; *n*-hexane, 2.0; cyclohexane, 4.4. Finally, the concentrations used in the comparative investigations presented in section 2A increase in the order $CH_2ICH_2I < CF_2ICF_2I < CF_2BrCF_2I$ (the optical densities of the samples were kept identical). If cluster formation were responsible for the production of I_2, a significant amount of I_2 would be observed also from CF_2BrCF_2I, in contrast to the actual observation.

To obtain further information about the mechanism for I_2 formation, we studied the excitation intensity dependence and concentration dependence of CH_2ICH_2I kinetics at 440 nm in acetonitrile. As shown in Figure 5, the shape of the kinetics does not vary with the excitation intensity and is independent of the solute concentration within the experimental error, indicating that the same mechanism(s) leading to I_2 formation dominates within the examined ranges ($I_0 = 1.8 \times 10^{14}$ to 1.7×10^{15} W/m^2; $C = 3.5$−26 mM) below 500 ps. The absence of a pronounced concentration dependence excludes a sequential cluster mechanism, because this mechanism would be favored by an increasing average size of the clusters.

SCHEME 1: Proposed Scheme for the Photodissociation of 1,2-Diiodoethane in Solution upon 266 nm Excitation[a]

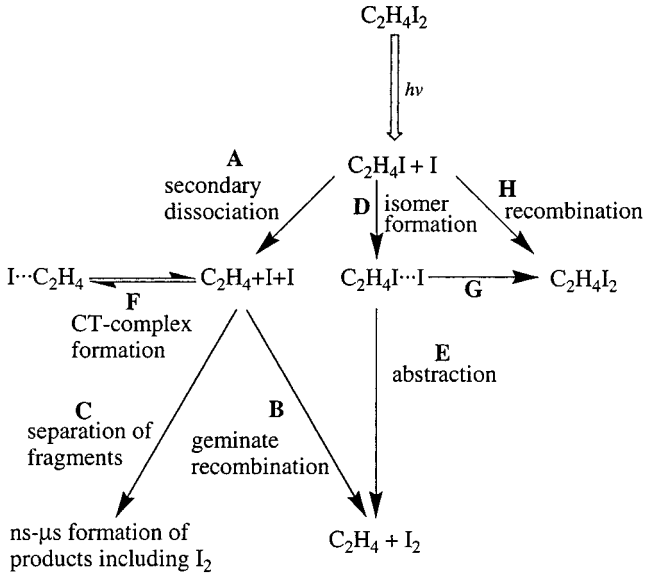

[a] Reaction paths A and B account for the major part of the observations below 500 ps, whereas C dominates on longer (nanosecond to microsecond) time scales (see section 3D). Reactions D−F are suggested to account for part of the observations below 500 ps (see section 3E). Reactions D−H are thought to be minor paths. A similar scheme is applicable for CF_2ICF_2I.

Only a one-photon process gives rise to I_2 formation in our experiments. This is concluded on the basis of the investigated intensity dependence of the signal amplitude at the probe wavelength 440 nm for CH_2ICH_2I in acetonitrile ($C = 12$ mM). An approximately linear increase of the signal amplitude at two delay times, 50 and 100 ps, was observed with increasing excitation intensity from 2×10^{14} to 2×10^{15} W/m^2. If the signal were due to absorption of two photons per CH_2ICH_2I from the pump pulse, deviation from linearity would have been observed, contrary to our observations.

By excluding other possibilities, the evidence presented in this section shows that fast formation of I_2 following excitation of CH_2ICH_2I or CF_2ICF_2I occurs by a cluster-independent mechanism initiated by one-photon absorption (Scheme 1). Most likely, this implies the mechanism proposed in section 3A: one-photon absorption yields vibrationally hot haloethyl radicals, which undergo secondary dissociation followed by geminate combination of iodine atoms. Another mechanism that we believe could accompany the aforementioned is iodine abstraction from the haloethyl radical by the liberated iodine atom. Because cage escape is expected to occur to some extent, more I_2 is expected to form on longer time scales, by nongeminate combination. This is investigated in the following section.

D. Vicinal Dihalides on the Nanosecond−Microsecond Time Scale. We measured the transient absorption on the nanosecond to microsecond time scale using the Nd:YAG laser system described in section 2 in order to obtain additional information about the formation of I_2 (e.g., quantum yields in different solvents for the three vicinal halides and occurrence of nongeminate formation) and the stability of haloethyl radicals.

The measurements presented in this section were performed in *n*-hexane, dichloromethane, and tetrachloromethane. Representative kinetics are shown in Figure 6. We do not present measurements in acetonitrile because I_3^- formation substantially complicates the kinetics in this solvent on the nanosecond to microsecond time scale. In all three solvents, I_2 formation was

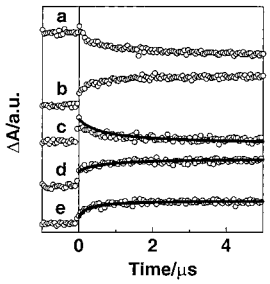

Figure 6. Transient absorption kinetics after excitation at 266 nm. From top: (). CH_2ICH_2I in tetrachloromethane at 290 nm; (b) CH_2ICH_2I in tetrachloromethane at 510 nm; (c) CH_2ICH_2I in *n*-hexane with fit at 330 nm; (d) CH_2ICH_2I in *n*-hexane with fit at 530 nm; (e) CF_2ICF_2I in *n*-hexane with fit at 530 nm. The concentrations used were 2.6 mM CH_2ICH_2I and 5.7 mM CF_2ICF_2I.

observed following excitation of both CH_2ICH_2I and CF_2ICF_2I at 266 nm. From the kinetic traces it can be seen that the formation of I_2 is biphasic: a fast resolution-limited rise is followed by a $\sim$1 μs rise. We determined the quantum yield of I_2 formation actinometrically using solutions of benzophenone in acetonitrile, which upon excitation at 266 nm forms a triplet ($\epsilon_{520nm} = 5800\ M^{-1}\ cm^{-1}$ in acetonitrile[46]) with unity quantum yield. From kinetics measured close to the I_2 absorption maximum, the final quantum yield for I_2 formation was determined to be 1.0 $\pm$ 0.1 for CH_2ICH_2I in all solvents examined. The corresponding values for CF_2ICF_2I were slightly lower: 0.75$-$0.95. The quantum yields for photodestruction of parent molecules (determined from the bleach at 290 or 280 nm in tetrachloromethane, see curve "a" of Figure 6) were equal to the yield of I_2 for both CH_2ICH_2I and CF_2ICF_2I. From this we conclude that photodissociation of the haloethyl radicals is negligible at the excitation intensities employed and that a small fraction of $^{\bullet}CF_2CF_2I$ recombines with I atoms. Furthermore, because the ratio between the fast and slow phases of molecular iodine formation is higher (by approximately a factor of 3 in *n*-hexane, cf. Figure 6d,e) for CH_2ICH_2I than for CF_2ICF_2I, it is reasonable to assume that the dominant mechanism for I_2 formation during the faster phase is the same in the femtosecond to picosecond experiments as in the nanosecond to microsecond experiments. Indirectly, this supports our argument that clusters play no role for the formation of I_2, because the concentrations employed in the nanosecond to microsecond experiments were comparatively low (10 mM for CF_2BrCF_2I and less for the two other compounds; see Figure 6).

It seems reasonable to assign the slower rise mainly to combination of iodine atoms having escaped the solvent cage. This assignment is supported by the fact that the rise in hexane could be well fitted (see Figure 6c$-$e) using second-order kinetics:

$$\Delta A(t) = A[I]_0^2/(1/kt + [I]_0) \qquad (2)$$

with $k = 1.3 \times 10^{10}\ M^{-1}\ s^{-1}$, which equals the previously determined rate constant for the reaction $2I \rightarrow I_2$ in *n*-hexane.[47] $[I]_0$, the initial concentrations of "free" iodine atoms was set to $[I]_0 = 1.2 \times 10^{-4}$ M for CH_2ICH_2I and $[I]_0 = 3 \times 10^{-4}$ M for CF_2ICF_2I. These concentrations were close to those obtained from the "final" I_2 concentrations estimated using the Lambert$-$Beer law. The steady-state absorption spectrum of I_2 has a low amplitude between 290 and 350 nm. Therefore, the contribution of I_2 to the transient absorption can be neglected in this spectral region. In this region, a submicrosecond decay was observed, as shown for 330 nm in Figure 6c. This decay was also fitted using the same rate constant and concentration parameters as used for fitting the rise of I_2. Similar decays of lower amplitude were observed in the same spectral region in both tetrachloromethane and dichloromethane. When we subtract the transient absorption signal at 10 μs (essentialy the bleach contribution) from that at 50 ns, we obtain a spectrum that is in close agreement with a previously published spectrum of I-atom:*n*-hexane charge-transfer absorption.[48] The decay we observe in hexane after subtraction of ΔA at 10 μs is approximately uniform in the range 290$-$350 nm, showing that I-atom:*n*-hexane CT absorption and parent bleach are the only significant contributions after 50 ns. Therefore, our analysis indicates that haloethyl radicals do not contribute to the transient absorption in the range 290$-$350 nm at times longer than 50 ns. The primary reason for this is most likely, considering the high quantum yields of I_2 formation and the facts that both the time evolution of the signal and its "final" level can be explained without assuming that haloethyl radicals give a contribution to the signal after 50 nm, that the lifetimes of these radicals are shorter than 50 ns; whether they have significant absorption in this spectral region is uncertain (see section E). Regarding this issue, a conclusive analysis of data at time delays shorter than 50 ns is precluded due to the presence of scattered excitation light in traces measured below 310 nm and signal-to-noise limitations.

CF_2BrCF_2I was examined in dichloromethane. The kinetics were relatively complex (data not shown) and suggest the presence of I_2, IBr, and Br_2 already after $\sim$50 ns, indicating that secondary dissociation occurs to a substantial extent for this compound. In this context it should be mentioned that Scaiano and co-workers,[49] also using actinometry in a nanosecond photolysis experiment, determined that 266 nm excitation of CH_2BrCH_2Br in acetonitrile solution yields bromine atoms with a quantum yield of 2.

E. Spectral assignments. *Haloethyl Radicals.* Obviously, knowledge of the absorption spectra of haloethyl radicals would be useful for determining their lifetime. However, we have found no spectra of haloethyl radicals in the literature although it is known that the $^{\bullet}CF_2CF_2Br$ radical absorbs at 248 nm.[28] DFT calculations of Zheng and Phillips[50] indicate that the first two absorption bands of $^{\bullet}CH_2CH_2Br$ are located in the 280$-$300 nm region, a result that has some support from a nanosecond resonance Raman study.[51] A comparison between the experimental gas-phase spectrum of $^{\bullet}CH_2I$[52] with that of $^{\bullet}CH_2Br$[53] or that of CH_3I with that of CH_3Br indicates, by analogy, that the spectrum of $^{\bullet}CH_2CH_2I$ is red-shifted compared to that of $^{\bullet}CH_2CH_2Br$. It is therefore not unreasonable to assume that $^{\bullet}CH_2CH_2I$ (and also $^{\bullet}CF_2CF_2I$) contribute to the transient absorption in the blue part of the spectral region examined in section 2A. However, the absence of anisotropy in the transient absorption in CH_2ICH_2I in acetonitrile at 380 nm (not shown) suggests that the contribution due to $^{\bullet}CH_2CH_2I$ is small in this spectral region.

Recent ab initio calculations by Ihee et al. have shown that the stable structures of $^{\bullet}CH_2CH_2I$ and $^{\bullet}CH_2CH_2Br$ are bridged.[54] The calculations by Zheng and Phillips[50] pertain to an open structure and might therefore seem to be invalidated by this study. However, they could still apply to the initially formed haloethyl radicals because it is natural to assume that these are open. An ultrafast electron diffraction study on photodissociation of CF_2ICF_2I indicates the formation of the $^{\bullet}CF_2CF_2I$ radical having an open ("classical") structure on the picosecond time scale.[3,4] According to most recent ab initio calculations on isolated $^{\bullet}CF_2CF_2I$, the open structure is most stable.[55] Whether this is its energetically preferred structure in solution remains to be determined.

Interaction between Haloethyl Radicals and Iodine Atoms. Some of the primary released iodine atoms are, due to their large size, likely to remain in the solvent cage and interact with the C−X chromophore of the haloethyl radicals. In the following discussion, we will argue that these interactions can give rise to transient absorption in the visible spectral region (weak absorption bands observed around 400 nm for CH_2ICH_2I and CF_2ICF_2I and around 410−440 nm for CF_2BrCF_2I) by forming species analogous to H_2C-I-I (isodiiodomethane) and that this may promote C−X cleavage producing XI.

Intensive absorption in a broad band around 400 nm has been observed for both isodiiodomethane, H_2C-I-I, and alkyl halide: iodine CT complexes[56−59] $CH_3I-I^{\bullet}$ and $RI_2-I^{\bullet}$. Isodiiodomethane was discovered upon UV photolysis of diiodomethane in solid matrixes at low temperature,[9,10] and later, in the liquid-phase photodissociation studies of diiodomethane in acetonitrile[11,12] and other solvents[60] at room temperature. In acetonitrile, this species is relatively long-lived (lifetime is about 200 ns) and has its largest absorption maximum at 390 nm with $\epsilon = 5600$ M^{-1} cm^{-1}.[12] Low-energy excitation (266 nm) of diiodomethane results in C−I bond breaking, the produced radicals form H_2C-I-I in a cage of acetonitrile molecules with the quantum efficiency of about 70%.[12] Substituting a C−Br bond for the C−I bond red shifts the isomer transition without significant change of absorption intensity and shortens the isomer lifetime.[9,10,12]

The transient absorption in acetonitrile solutions at 400 nm is at all time delays considerably higher for CH_2I_2 than for CH_2ICH_2I (e.g., 17 times at 50 ps; Figure 2 and section 3A). Nevertheless, formation of analogous species after dissociation of vicinal dihalomethanes (we refer to them as isodihaloethanes) probably occurs, although with a much smaller quantum yield due to competing secondary dissociation and the greater separation between the iodine atoms in the parent molecule. Also due to secondary dissociation, the quantum yield for formation of $I-BrCF_2CF_2$ and $I-ICF_2CF_2$ can be expected to be higher than that of $I-ICH_2CH_2$. As seen in Figure 3, the signal amplitude at early time delays at 440 nm is higher for both CF_2BrCF_2I and CF_2ICF_2I than for CH_2ICH_2I, despite the fact that vibrationally hot I_2 gives a larger contribution at early time delays for CH_2ICH_2I. A contribution from isodihaloethanes to the transient absorption at this wavelength provides an explanation to this fact. Moreover, it can also explain the presence of decays in the transient absorption traces for CH_2ICH_2I and CF_2ICF_2I (5−6 ps) and CF_2BrCF_2I (∼100 ps). Decay of isodihaloethanes should be expected to be faster than isodihalomethanes (due to the formation of stable products following C−X cleavage in the former case) and occur faster the weaker the C−X bond. On the basis of the weak intensity of these bands, the quantum yield of isomerization of the vicinal dihaloethanes is estimated to be less than $^1/_{10}$th of the I_2 formation quantum yield for the corresponding dihaloethanes at a delay of 500 ps (assuming an extinction coefficient for isodihaloethanes of ∼6000 M^{-1} cm^{-1}, i.e., similar to that of the H_2C-I-I isomer).

Because the weak bands were observed early after excitation, the assignment of these bands to dihaloethane−iodine CT complexes is highly unlikely because formation of such a complex is controlled by diffusion, which occurs on a nanosecond time scale at the concentrations used.

I−Atom−Ethene CT Complexes. As seen in Figure 2, panel D, the transient spectrum of CH_2ICH_2I at 500 ps has a contribution from a species other than I_2 around 400 nm. According to the discussion in the previous paragraph, it cannot be due to $I-ICH_2CH_2$ because this species is not expected to be present at 500 ps and because no corresponding absorption for CF_2ICF_2I was observed. Instead, we assign this absorption to charge-transfer interaction between iodine atoms and ethene, the product formed after secondary dissociation. The absorption maximum for this charge-transfer complex ($I:C_2H_4$ CTC) was calculated to 399 nm, using experimental data from the ethyne−iodine charge-transfer complex[61] and the difference in ionization potentials[62] between ethyne (11.4 eV) and ethene (10.51 eV) and assuming that the Coulomb terms are the same for the CT states in the two systems.

4. Conclusions

The photodissociation dynamics of CH_2ICH_2I, CF_2ICF_2I, and CF_2BrCF_2I have been studied in acetonitrile solution after excitation at 266 nm. Within tens of picoseconds, formation of I_2 was observed from CH_2ICH_2I and CF_2ICF_2I, but not from CF_2BrCF_2I. Following excitation of CH_2ICH_2I, ultrafast I_2 formation was observed in several other solvents (dichloromethane, tetrachloromethane, cyclohexane, and *n*-hexane). We propose that the predominant mechanism for I_2 formation is secondary dissociation of the haloethyl radicals followed by geminate combination of iodine atoms. For CF_2ICF_2I, in particular, where direct comparison is possible with gas-phase time-resolved studies, our results (including both femtosecond and nanosecond experiments) indicate that the haloethyl radicals are not more long-lived than in the gas phase, despite the possibility of vibrational cooling by the solvent. Various other pieces of evidence, including intensity and concentration dependence of kinetics, show that photodissociation of haloethyl radicals or cluster-dependent mechanisms do not play an important role in the formation of I_2. In nanosecond laser photolysis experiments, we determined the final quantum yields for I_2 formation on the microsecond time scale to be 1 ± 0.1 for CH_2ICH_2I and 0.85 ± 0.1 for CF_2ICF_2I in *n*-hexane, dichloromethane, and tetrachloromethane. The nanosecond to microsecond data indicate that all haloethyl radicals decay within tens of nanoseconds. We argue that the decay of haloethyl radicals can partially occur via abstraction. The various reaction paths leading to I_2 formation following photoexcitation of a vicinal dihalide are depicted in Scheme 1.

Acknowledgment. We thank Dr. Jennifer L. Herek for valuable comments on the manuscript and Dr. Bengt Nelander for fruitful discussions. The work was supported by the Swedish Science Research Council, Trygger Foundation, Magnus Bergwall Foundation, Knut and Alice Wallenberg Foundation, and Crafoord Foundation.

References and Notes

(1) Khundkar, L. R.; Zewail, A. H. *J. Chem. Phys.* **1990**, *92*, 231.
(2) Zhong, D.; Ahmad, S.; Zewail, A. H. *J. Am. Chem. Soc.* **1997**, *119*, 5978.
(3) Cao, J.; Ihee H.; Zewail, A. H. *Proc. Natl. Acad. Sci. U.S.A.* **1999**, *96*, 338.
(4) Ihee, H.; Lobastov, V. A.; Gomez, U. M.; Goodson, B. M.; Srinivasan, R.; Ruan, C.-Y.; Zewail, A. H. *Science* **2001**, *291*, 458.
(5) Nathanson, G. M.; Minton, T. K.; Shane, S. F.; Lee, Y. T. *J. Chem. Phys.* **1989**, *90*, 6157.
(6) Minton, T. K.; Felder, P.; Brudzynski, R. J.; Lee, Y. T. *J. Chem. Phys.* **1984**, *81*, 1759.
(7) Minton, T. K.; Nathanson, G. M.; Lee, Y. T. *J. Chem. Phys.* **1987**, *86*, 1991.
(8) Gerck, E. *J. Chem. Phys.* **1983**, *79*, 311.
(9) Maier, G.; Reisenauer, H. P. *Angew. Chem., Int. Ed. Engl.* **1986**, *25*, 819.
(10) Maier, G.; Reisenauer, H. P.; Hu, J.; Schaad, L. J.; Hess, A. B., Jr. *J. Am. Chem. Soc.* **1990**, *112*, 5117.

(11) Tarnovsky, A. N.; Alvarez, J.-L.; Yartsev, A. P.; Sundström, V.; Åkesson, E. *Chem. Phys. Lett.* **1999**, *312*, 121.
(12) Tarnovsky, A. N.; Wall, M.; Rasmusson, M.; Sundström V.; Åkesson, E. In *Femtochemistry and Femtobiology. Ultrafast Dynamics in Molecular Science*; Douhal, A., Santamaria, J., Eds.; World Scientific: Singapore, 2002, p 247.
(13) Carter, E. A.; Goddard, W. A., III. *J. Chem. Phys.* **1988**, *88*, 3132.
(14) Owrutsky, J. C.; Raftery, D.; Hochstrasser, R. M. *Annu. Rev. Phys. Chem.* **1994**, *45*, 519.
(15) Zheng, X.; Cheng, Y. F.; Phillips, D. L. *Chem. Phys. Lett.* **1998**, *292*, 295.
(16) Wang, G.-J.; Zhang, H.; Zhu, R.-S.; Han, K.-L.; He, G.-Z.; Lou, N.-Q. *Chem. Phys.* **1999**, *241*, 213.
(17) Åberg, U.; Åkesson, E.; Alvarez, J.-L.; Fedchenia, I.; Sundström, V. *Chem. Phys.* **1994**, *183*, 269.
(18) Tarnovsky, A. N.; Wall, M.; Rasmusson, M.; Pascher, T.; Åkesson, E. *J. Chin. Chem. Soc.* **2000**, *47*, 769 (Special Issue).
(19) Rasmusson, M.; Tarnovsky, A. N.; Åkesson, E.; Sundström, V. *Chem. Phys. Lett.* **2001**, *335*, 201.
(20) Kovalenko, S. A.; Dobryakov, A. L.; Ruthmann, J.; Ernsting, N. P. *Phys. Rev. A* **1999**, *59*, 2369.
(21) Ekvall, K.; van der Meulen, P.; Dhollande, C.; Berg, L.-E.; Pommeret, S.; Naskrecki, R.; Mialocq, J.-C. *J. Appl. Phys.* **2000**, *87*, 2340.
(22) Popov, A. I.; Deskin, W. A. *J. Am. Chem. Soc.* **1958**, *80*, 2976.
(23) Johnson, A. E.; Myers, A. B. *J. Phys. Chem*, **1996**, *100*, 7778.
(24) The choice of acetonitrile as the main solvent for studying the photoinduced reaction dynamics of haloethanes is motivated by the relatively small transient absorption signal of neat acetonitrile after excitation at 266 nm.
(25) Sukowski, U.; Seilmeier, A.; Elsaesser, T.; Fischer, S. F. *J. Chem. Phys.* **1990**, *93*, 4094.
(26) Elsaesser, T.; Kaiser, W. *Annu. Rev. Phys. Chem.* **1991**, *42*, 83.
(27) Pence, W. H.; Baughcum, S. L.; Leone, S. R. *J. Phys. Chem.* **1981**, *85*, 3844.
(28) Krajnovich, D.; Butler, L. J.; Lee, Y. T. *J. Chem. Phys.* **1984**, *81*, 3031.
(29) Two iodine atoms at a distance l and separated by the solvent find each other on a characteristic time scale t, $t \approx l^2/D$, where D is relative diffusion coefficient of I atoms. For acetonitrile at 20 °C, $D \sim 9 \times 10^{-5}$ cm^2 s^{-1}. This estimate is based on the Stokes−Einstein equation, $D_I = k_b T/4\pi\eta r_I$, with $\eta \approx 0.36$ cP, $r_I \approx 2.2$ Å, and $D = 2D_I$). The distance $l \approx 130$ Å for the experimental conditions of Figure 2 yields $t \approx$ 20 ns.
(30) Lienau, C.; Zewail, A. H. *J. Phys. Chem.* **1996**, *100*, 18629.
(31) Berg, M.; Harris, A. L.; Harris, C. B. *Phys. Rev. Lett.* **1985**, *54*, 951.
(32) Harris, A. L.; Berg, M.; Harris, C. B. *J. Chem. Phys.* **1986**, *84*, 788.
(33) Smith, D. E.; Harris, C. B. *J. Chem. Phys.* **1987**, *87*, 2709.
(34) Harris, A. L.; Brown, J. K.; Harris, C. B. *Annu. Rev. Phys. Chem.* **1988**, *39*, 341.
(35) Our UV−vis absorption measurements.
(36) Contribution of the solvent signal to the measured transient absorption signal depends on solute concentration because of reduction of excitation beam intensity due to solute absorption. The solvent contribution can be reasonably estimated provided that intensity dependencies of the signal from neat solvent is known, e.g. ,measured with neutral density filters prior to adding the solute.
(37) Control measurements described in the section 2 emphasize the absence of I_2 as contaminant to the signal.
(38) Waschewsky, G. C. G.; Horansky, R.; Vaida V. *J. Phys. Chem.* **1996**, *100*, 11559.
(39) Roehl, C. M.; Burkholder, J. B.; Moortgat, G. K.; Ravishankara, A. R.; Crutzen P. J. *J. Geophys. Res.* **1997**, *102*, 12819.
(40) Fan, Y. B.; Randall, K. L.; Donaldson, D. J. *J. Chem. Phys.* **1993**, *98*, 4700.
(41) Zhong, D.; Zewail, A. H. *J. Phys. Chem. A* **1998**, *102*, 4031.
(42) Syage, J. A. *Chem. Phys.* **1996**, *207*, 411.
(43) Ito, F.; Nakanaga, T.; Futami, Y.; Kudoh, S.; Takayanagi, M.; Nakata, M. *Chem. Phys. Lett.* **2001**, *343*, 185.
(44) Naitoh, Y.; Inoue, Y.; Yoshihara, K. In *Femtochem. IV, Book Abstr.* **1999**, 253.
(45) Donaldson, D. J.; Vaida, V.; Naaman, R. I. *J. Chem. Phys.* **1987**, *87*, 2522.
(46) Bensasson, R. V.; Gramain, J.-C. *J. Chem. Soc., Faraday Trans. 1* **1980**, *76*, 1801.
(47) Marshall, R.; Davidson, N. *J. Chem. Phys.* **1953**, *21*, 2086. Aditya, S.; Willard, J. E. *J. Am. Chem. Soc.* **1957**, *79*, 2680.
(48) Logan, S. R.; Bonneau, R.; Joussot-Dubien, J.; Fornier de Violet, P. *J. Chem. Soc., Faraday Trans. 1* **1975**, *7*, 2148.
(49) Scaiano, J. C.; Barra, M.; Krzywinski, M.; Sinta, R.; Calabrese, G. *J. Am. Chem. Soc.* **1993**, *115*, 8340.
(50) Zheng, X.; Phillips, D. L. *J. Phys. Chem. A* **2000**, *104*, 1030.
(51) Zheng, X.; Phillips, D. L. *J. Chem. Phys.* **1999**, *110*, 1638.
(52) Sehested, J.; Ellermann, T.; Nielsen, O. J. *Int. J. Chem. Kinet.* **1994**, *26*, 259.
(53) Villenave, E.; Lesclaux, R. *Chem. Phys. Lett.* **1995**, *236*, 376.
(54) Ihee, H.; Zewail, A. H.; Goddard, W. A., III. *J. Phys. Chem. A* **1999**, *103*, 6638.
(55) Ihee, H.; Kua, J.; Goddard, W. A., III; Zewail, A. H. *J. Phys. Chem. A* **2001**, *105*, 3623.
(56) Mittal, J. P.; Hamill, W. H. *J. Am. Chem. Soc.* **1967**, *89*, 5749.
(57) Strong, R. L.; Kaye, J. A. *J. Am. Chem. Soc.* **1976**, *98*, 5460.
(58) Shoute, L. C. T.; Neta, P. *J. Phys. Chem.* **1991**, *95*, 4411.
(59) Miranda, M. A.; Pérez-Prieto, J.; Font-Sanchis, E.; Scaiano, J. C. *Acc. Chem. Res.* **2001**, *34*, 717.
(60) Tarnovsky, A. N.; Sundström, V.; Åkesson, E. Manuscript in preparation.
(61) Engdahl, A.; Nelander, B. *Chem. Phys. Lett.* **1984**, *106*, 527.
(62) *CRC Handbook of Chemistry and Physics*, 80th ed.; CRC Press LLC: Boca Raton, FL, 1999.